Morphology of Porous Silicon Nanostructures in p-type Silicon Based on Novel Comparison between Two Electrochemical Cells Design

Zainab Abduljabbar Yaseen[1], Ghadah Abdaljabar Yiseen[2,*]

[1] Electrical and Electronic Engineering department, Fatih University, Istanbul, Turkey ,
[2] Department of Chemistry, College of Science, University of Baghdad, Baghdad,
[*]E-mail: ghadah.yiseen@scbaghdad.edu.iq, ghadah.yiseen@yahoo.com

Two electrochemical cells design (designed single tank cell and double tank cell) with three specific alcoholic solvents at constant anodization time and current density have been utilized to perform anodization in p-type silicon to prepare porous silicon nanostructures. Morphology and pore formation of porous silicon layers were characterized by Atomic Force Microscopy (AFM) and current-voltage (I-V) measurement, photoluminescence emission by ultraviolet-lamp (254-366)nm, three main types of pores could be obtained for both cells; mesopores, mesopore fill of mesopores, and macropore fill of mesopores. Single tank cell has been differentiated from double tank cell in showing stable red-orange ultraviolet photoluminescence emission increases with increasing carbon numbers in the alcohol with an improvement in current–voltage measurement.

1. INTRODUCTION

Porous silicon (PS) is a nanostructured material prepared by various chemical and electrochemical etching processes in hydrogen fluoride (HF) solution [1]. The electrochemical etching cell has been designed and made in various ways in the past [1]. The most common electrolytic single cell used in the production of porous silicon layers (PSLs) is very simple and based on the technique originally used by Uhlir [2,3]. Another type of etching cell consists in a double tank in which the electrolyte of one of the tanks is used as a back side contact of the silicon wafer [3,4]. Careful design of the electrochemical cell is required to achieve good lateral film uniformity [5, 6]. A number of

factors; such as the type and doping level of the silicon substrate, the electrochemical parameters, and solution composition determine the pore morphologies dramatically [9]. According to current definitions from the International Union of Pure and Applied Chemistry (IUPAC) [10], porous structures are typically sorted into three categories by the size of the pores: micropores (<2 nm), mesopores (2-50 nm), and macropores (>50 nm) [9, 10].

For micro or mesoporous silicon formation, an electrolyte usually contains alcohol as a solvent; the effect of the presence of alcohol has been considered that it helps to reduce the surface tension or to keep away from coverage of H_2 bubbles on the porous layer, alcohol has also became to be used for macropore formation [11]. The effect of organic solvents has been discussed from various points of view over the years; it has been shown that some organic solvents can act as a mild oxidizing reactant for silicon [11-13]. All three kinds of pores have found their numerous applications in energy micro-sources [9] (Micro-fuel cells, micro- supercapacitors, Li-ion battery anodes) [9,10], photonic crystals [14,15], sacrificial layers [16,17], Bragg reflectors [18,19], solar cells [20,21], and biological applications [9,22–24].

The ultraviolet (UV) photoluminescence (PL) emission in PS has been extensively studied [31]. PL emission in p-type PS is usually in the near-infrared and visible regions [25-28]. Thus, in order to achieve UV luminescence emission in p-type PS, various post treatments should be involved including thermal oxidization or HF etching procedures [29-31]. And the performance of UV PL emission in the post-treated PS is yet unstable, the stable UV luminescence in proper PS is of great importance for applications [31]. This study concentrates on highlighting the functional difference between two electrochemical cells design (designed single tank cell and double tank cell) through different alcoholic solvents with constant anodization time and current density on the formation of porous silicon nanostructures in p-type silicon. The morphology of PS samples (pore size and type) were examined by Atomic force microscopy (AFM) whereas the electrical property by I-V characterization. The UV PL emission of PS was tested by a UV- lamp at (254-366) nm wavelength. UV PL emission at about 254nm and 366nm could be seen by naked eye and has been achieved with both cells design with a notable difference in UV emission and its stability in designed single tank cell in compare with the double tank cell.

2. EXPERIMENTAL

Two electrochemical etching cells (designed single tank and double tank cells) as can be seen in figure (1) were utilized to perform anodization of highly doped p-type, Si (100), boron doped, resistivity of (1-10 Ω cm) substrates in order to prepare porous silicon , the etching surface area that was exposed to the electrolyte; for double tank cell is $0.785cm^2$, whilst for designed single tank cell is $6.15cm^2$, in that respect the silicon wafer cut in two different areas: 1cmx1cm and 2cmx2cm, for double tank cell and designed single tank cell, respectively. The silicon wafers were cleaned with absolute ethanol and deionized water for 3 min, an ethanolic solution containing 1% HF was used to remove the native SiO_2 [7], the anodization electrolytes consisted of an alcoholic 48wt% hydrofluoric acid mixture; at ratio (1:1) in volume, with the following alcohols: 99.8wt% ethanol (C_2H_5OH),

99.8wt% methanol (CH_3OH) and 99.8wt% 2-propanol ($CH_3CHOHCH_3$) under constant current density 30 mA/cm^2 [7] provided by current source Keithley 200-60-2 (Programmable DC power supply. 60 V, 2.5 A, 1 channel, USB, GPIB for 60 min of anodization time. After the anodization; porous silicon samples rinsed with methanol many times and dried with pentane. Pentane has a much lower surface tension than either methanol or ethanol, and has been shown to reduce PS cracking during drying [8].
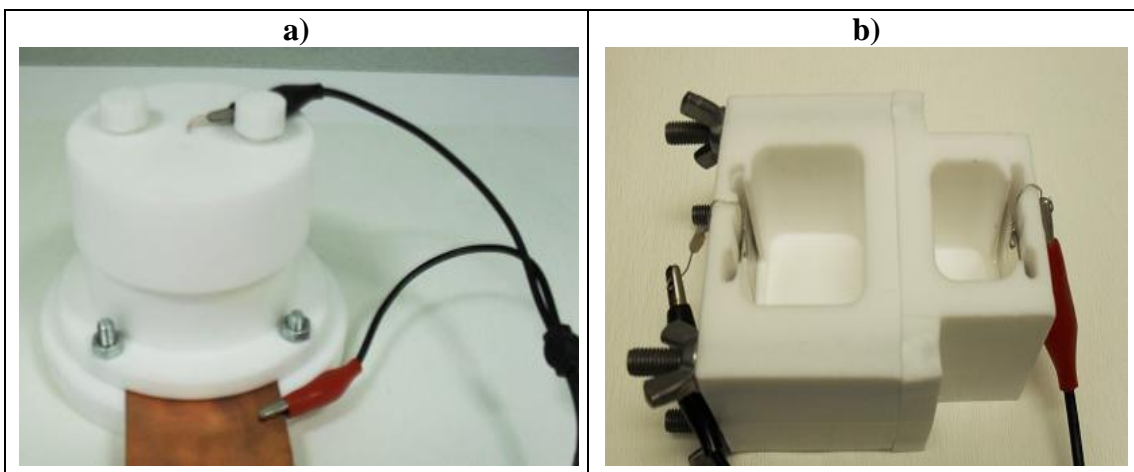

Figure 1. Experimental set-up of (a) the home-made Teflon single cell, and (b) double tank cell.

Atomic Force Microscopy (AFM XE-100 Park Systems) was used to investigate the pore formation and the morphology of porous silicon samples, Keithley Semiconductor characterization system model 4200-scs was used to measure current-voltage characteristics, the ultraviolet photoluminescence emission of porous silicon was tested by a UV- lamp at (254-366) nm wavelength.

3. RESULTS AND DISCUSSION

3.1 Atomic Force Microscopy

The morphology of PS samples (pore size and type) examined by Atomic force microscopy (AFM). Figure 2(a)-(c), figure 3 (a)-(b) and figure 4 (a)-(c) show three dimensional AFM images (500 nm x 500 nm) of porous silicon layers with three specific alcoholic solvents at constant etching time 60min and current density 30mA/cm^2 with two electrochemical cells design. It can be found that the surface was covered with a dense porous layer of hillocks and holes [36]. AFM can determine the surface nature of samples under contact mode employing section analysis [32]. Section analysis analyzes a profile of the scanning area of the sample, revealing the undulating vertical distance and surface roughness along the section, and thus measures the diameter and depth of pores [32-35].
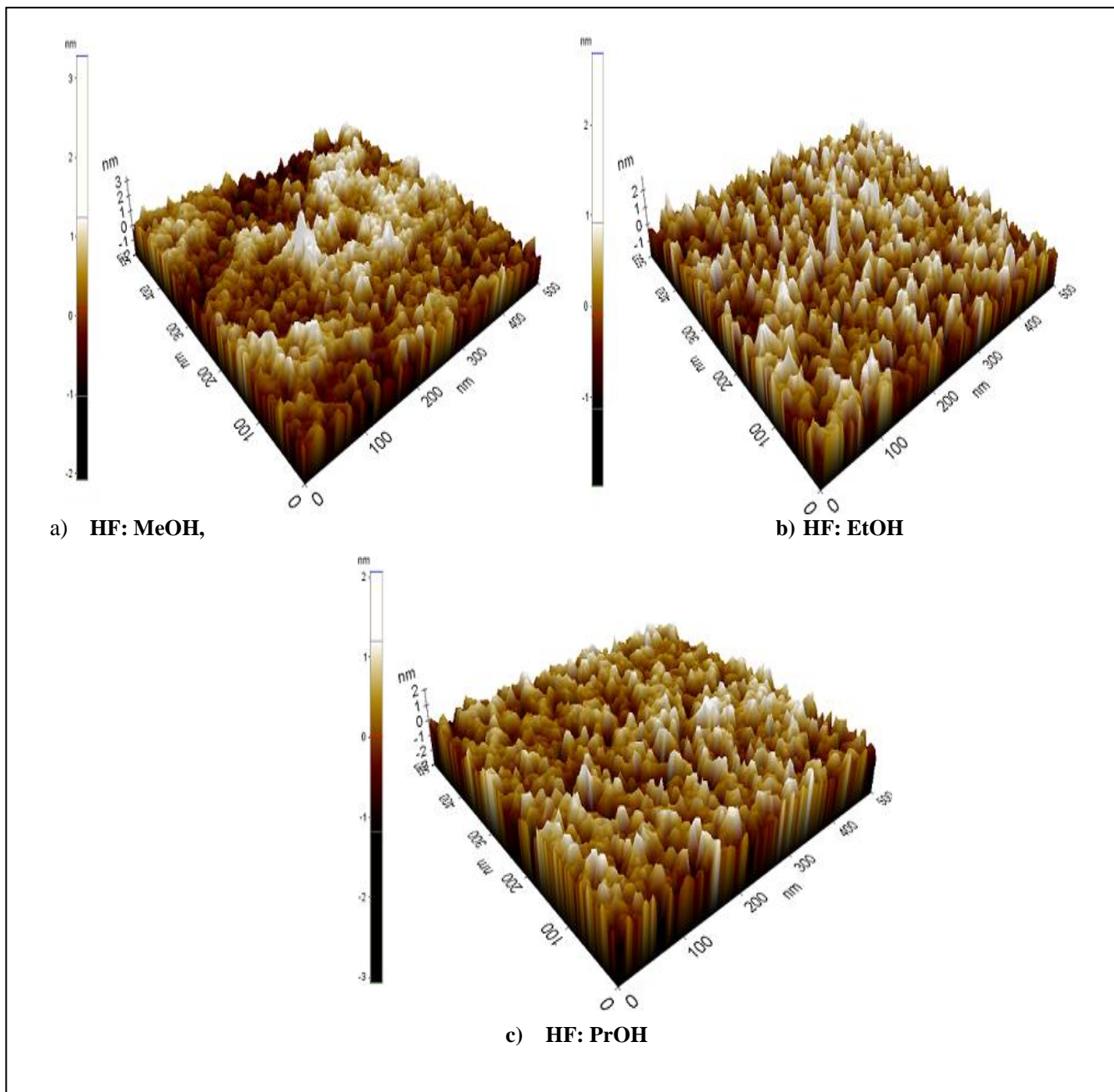
Figure 2. 3-D AFM image of PS layer in Single tank Cell, at etching time 60 min. with different alcoholic etching solvents used : (a)HF: MeOH, (b) HF:EtOH, and (c) HF:PrOH , at ratio (1:1) in volume.

When a 3D-image of PS layer was observed with AFM, there was a difference of surface levels between the original wafer surface and the top surface of anodized part. The dissolution behavior of the top surface varies depending on the type of alcohol [11]. Fig. 2(a)-(c): Shows the morphology of PS layer anodized for 60 min in 48 wt. % HF solution with MeOH, EtOH and PrOH by using *designed single tank cell* . It can be found that the diameters and depths of pores when MeOH is used as solvent were: *meso pores* between (9-30) nm, and (0.13-1) nm, respectively.

With EtOH , the diameters and depths of pores were: *meso pores* between (9-37)nm, and (0.3-1.25)nm, respectively; *meso pores fill of meso pores* between (24-45)nm , and (1.25-1.63)nm, respectively; and *macro pore fill of meso pores* (63)nm, and (0.9)nm, respectively. The depths of dissolved part at the top surface and porous layer depend on the type of alcohol [11]. The polarity and the surface tension of alcohol become lower with the increasing number of carbon in alcohol [11].


a) Rq. (0.518nm)   b) Rq. (0.231nm)
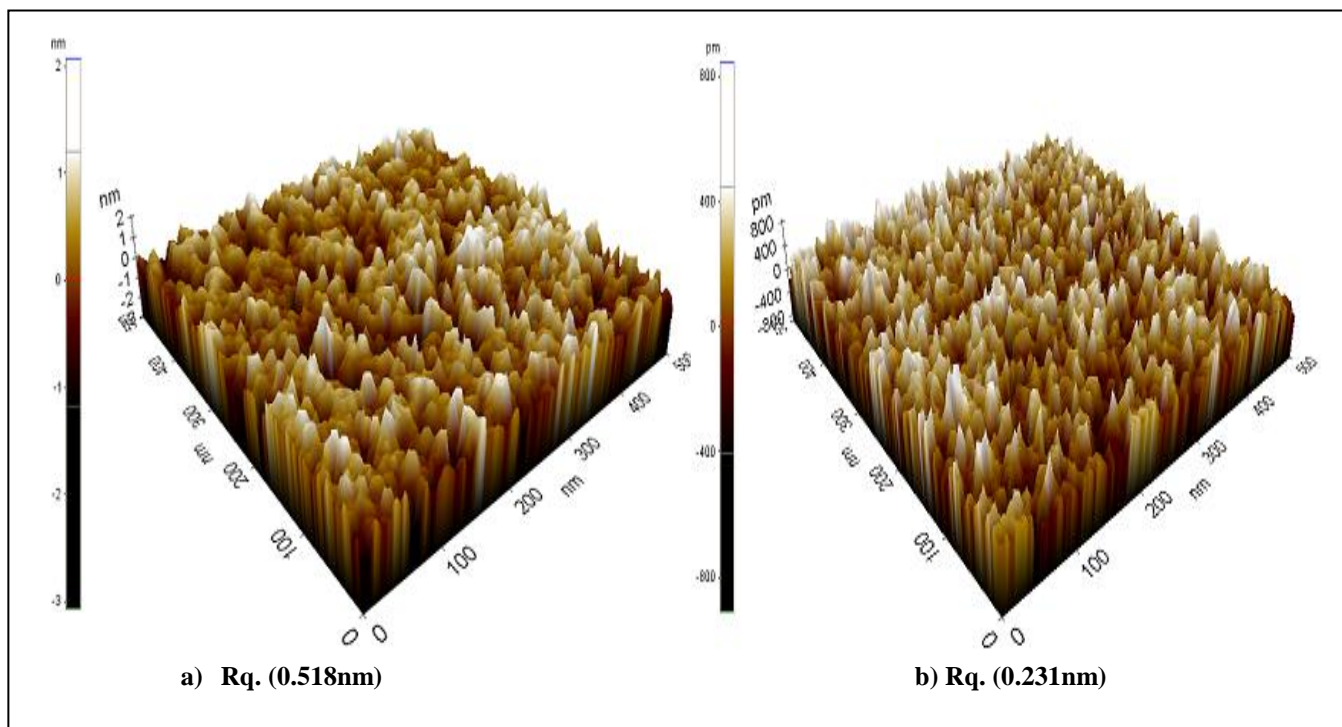
Figure 3. 3-D AFM image of PS two layers in Single tank cell, etched with HF: PrOH at ratio (1:1) in volume at etching time 60minute.

Surprisingly, fig. 3(a)-(b): Shows two different layers of porous silicon PS with two different surface roughness (Rq.) (a) 0.518nm and (b) 0.231nm. When PrOH is used as solvent, the diameters and depths of pores obtained from fig. 3(a) were: *meso pores* between (6-27)nm, and (0.13-1)nm, respectively; *meso pore fill of meso pores* (40)nm, and (0.63)nm, respectively. While the diameters and depths of pores obtained from fig.3 (b) were: *meso pores* between (9-22) nm, and (0.1-0.5) nm, respectively; *meso pores fill of meso pores* (23-31) nm, and (0.2-0.51) nm, respectively. PrOH has the highest viscosity at room temperature and the lowest surface tension [42] among EtOH and MeOH. Also, PrOH is considered as a proper solvent material to help form a homogeneous-etched surface[42].In particular, the porosity increased with decreased surface roughness and the stability of porous layers increases with the increasing carbon numbers in the alcohol at constant etched time [11-13] [42].
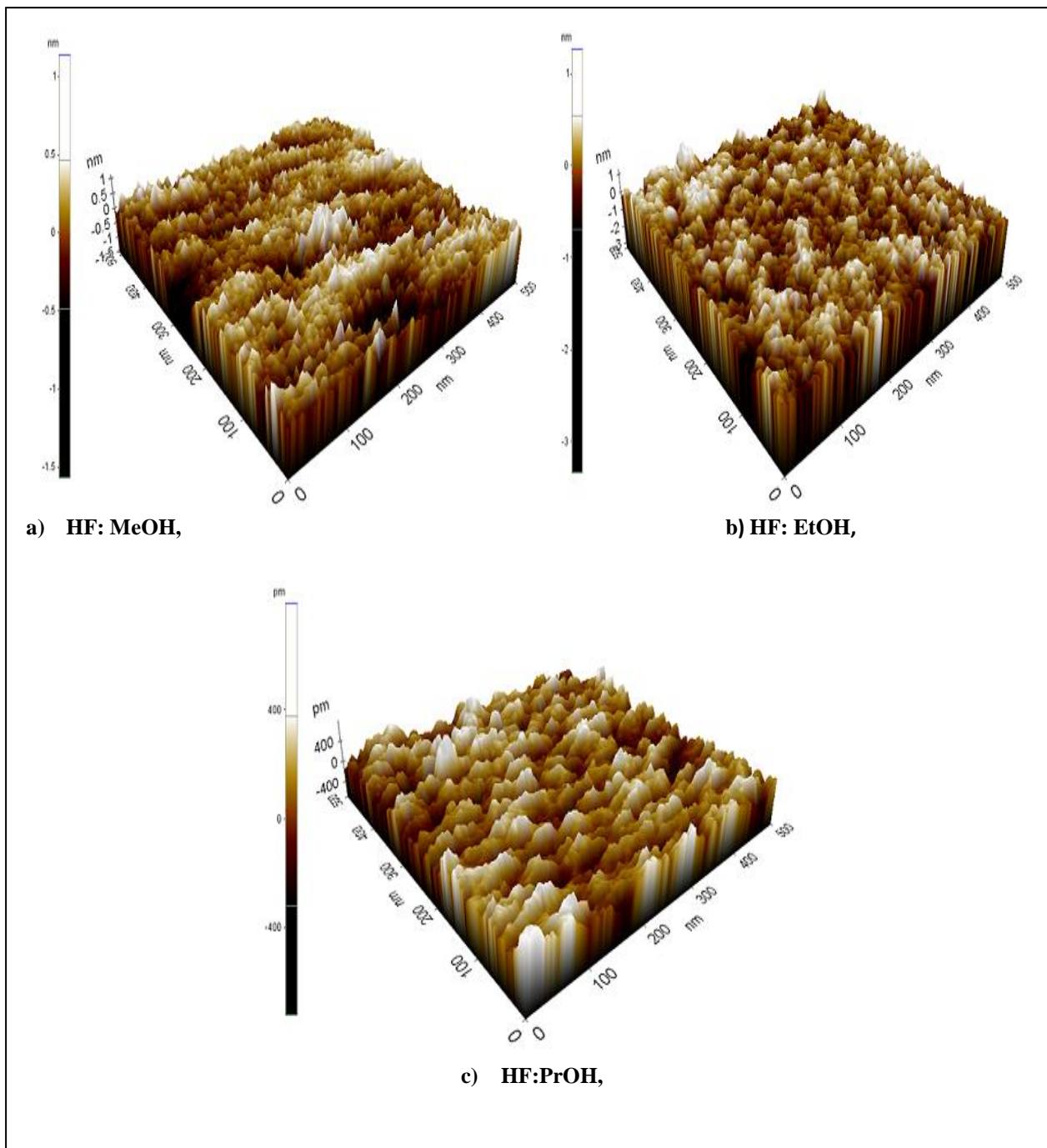
Figure 4. 3-D AFM image of PS layer in Double tank Cell, at etching time 60 min. with different alcoholic etching solvents used : (a)HF: MeOH, (b) HF:EtOH, and (c) HF:PrOH , at ratio (1:1) in volume.

Fig.4 (a)-(c): Shows the morphology of PS layer which anodized by using *double tank cell*. We have found that the diameters and depths of pores when MeOH is used as solvent were: *meso pores* between (7-26) nm, and (0.1-0.48) nm, respectively; *meso pores fill of meso pores* (45)nm, and (0.5)nm, respectively. With EtOH, the diameters and depths of pores are obtained *: meso pores* between (6-26)nm, and (0.1- 0.95)nm, respectively; *meso pores fill of meso pores* between (20-

34)nm, and (0.2- 0.51)nm, respectively; *macro pores fill of meso pores* between (52-55)nm, and (0.95-1)nm, respectively. When using PrOH, the diameters and depths of pores are obtained: *meso pores* between (6-32) nm, and (0.13-0.36)nm, respectively; *meso pore fill of meso* pores (25)nm, and (0.25)nm, respectively. In this study, fig.2 (a)-(c), fig. 3(a)-(b) and fig. 4(a)-(c) provided us with a clear demonstration about the effect of the etch cell engineering, which exert a profound influence on the formation of PS layers for constant anodization time with different alcoholic solvent.   For both etching cells, three main types of pores were obtained, in spite of the difference in the diameters and depths of pores were: mesopores, mesopore fill of mesopores, and macropore fill of mesopores [37], with spongy morphology were successfully produced using constant current density 30mA/cm^2 and constant anodization time 60 min by varying the composition of etching solvent 48 wt.% HF solution with the following alcohols MeOH, EtOH, and PrOH at ratio (1:1) in volume. The sensitivity of pore diameter to HF concentration strongly depends on solvent [37,38]. A wider range of pore diameters can be obtained in organic solvents than in aqueous solutions [37]. Jager et al. reported an interesting fact of the degree of filling of the macro pores formed on p-Si depends on the oxidizing nature of the solution[37]: macro pores are filled with micro PS in non-oxidizing electrolyte such as acetonitrile (MeCN), while they are not filled for oxidizing electrolytes such as dimethylformamide (DMF) [37]. In other words, macro pores formed in organic solvents tend to be more filled than those formed in aqueous solutions[37]. However, Walls of the macro pores are not always covered by a micro PS layer [37-41].

3.2 Ultraviolet Photoluminescence Emission of PS layer:

A significant stability of UV PL emission at (254-366) nm is achieved when p-type Si is anodized in three specific alcoholic solvents used: HF: MeOH , HF:EtOH, and HF:PrOH , at ratio (1:1) in volume, etched at 60 min. by using *designed single tank cell* as shown in table (1). From the above results obtained by AFM and table (1), PS samples exhibited clear and significant stable red-orange UV PL emission increases with increasing carbon numbers in the alcohol with slightly difference could be attributed to the diversity of type and size (diameter and depth) of pores obtained within the same cell with three specific alcoholic solvents; for MeOH were meso pores; for EtOH were meso pores, meso pores fill of meso pores and macro pore fill of meso pores; for PrOH were meso pores, meso pore fill of meso pores. The mesoporous layer exhibits a very rough texture, the mesoporous layer shows photoluminescence, whereas the macroporous layer does not [49].

Photoexcitation with blue or UV light generates confined electron–hole pairs in the nanocrystallites of porous silicon [7,50].whose dimensions are small enough to exhibit quantum confinement effects [26,51].Luminescence from PS is most frequently discussed in terms of a quantum confinement model [43]. As the characteristic size of a semiconductor is reduced to the nanometer regime, confinement of the electron and hole wave functions effectively increases the band gap of the material and hence the luminescence energy [52,53]. The energy of the luminescence to increase as the feature size is decreased [44].

Table 1. Shows the images of PS samples prepared by using designed single tank cell, under white light and UV (254-366) nm., with different alcoholic etching solvents used: HF: MeOH, HF:EtOH, and HF:PrOH , at ratio (1:1) in volume, etched at 60 min.

	White light	UV-254nm	UV-366nm
HF: methanol			
HF: ethanol			
HF: 2-propanol			
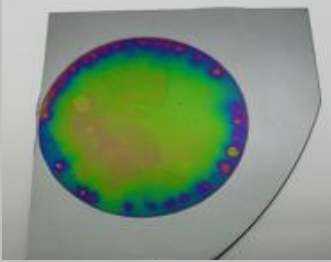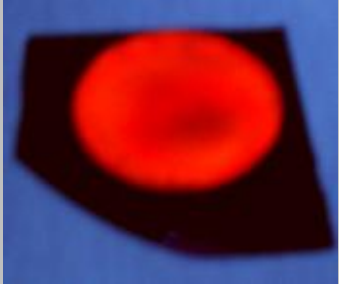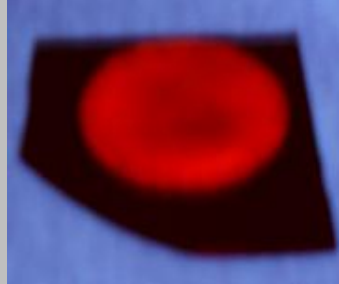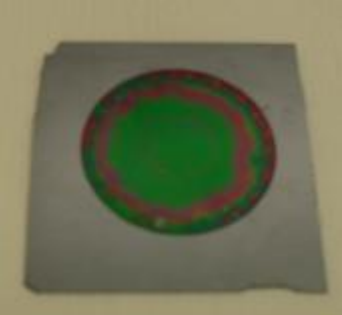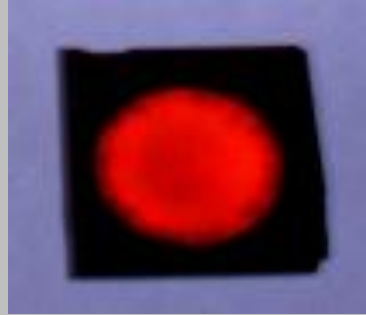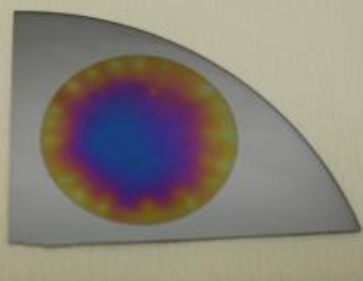
Table 2. Shows the images of PS samples prepared by using designed single tank cell and double tank cell, under white light and UV (254-366) nm., with HF:MeOH etching solvent at ratio (1:1) in volume, etched at 60 min.

	White light	UV-254nm	UV-366nm
Single Cell			

Double Cell		
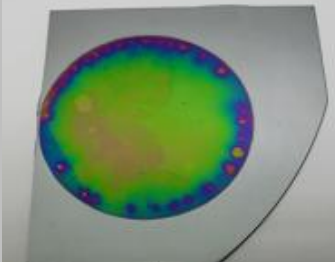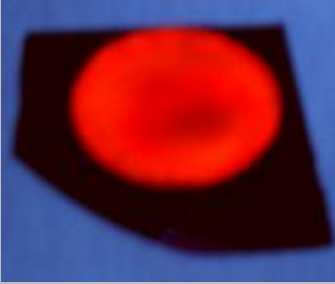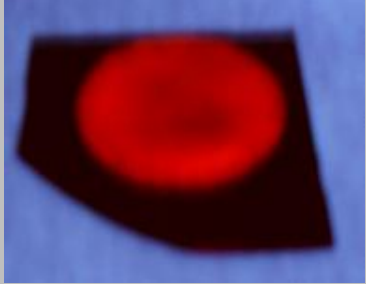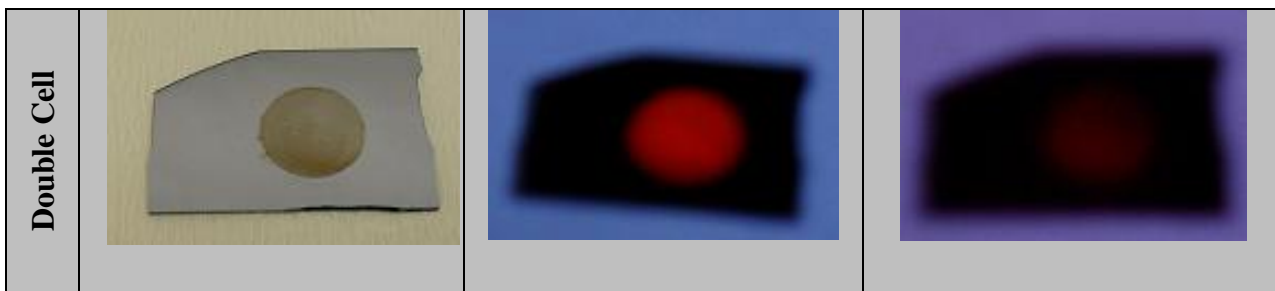
Table 3. Shows the images of PS samples prepared by using designed single tank cell and double tank cell, under white light and UV (254-366) nm., with HF:EtOH etching solvent at ratio (1:1) in volume, etched at 60 min.
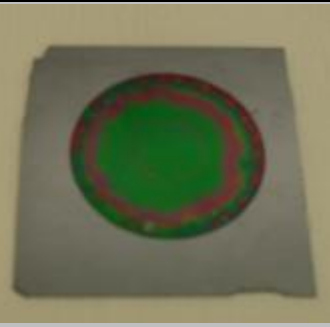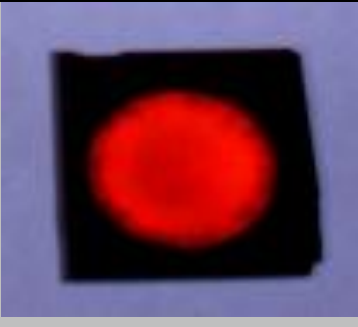
	White light	UV-254nm	UV-366nm
Single Cell			
Double Cell			none

Table 4. Shows the images of PS samples prepared by using designed single tank cell and double tank cell, under white light and UV (254-366) nm., with HF:PrOH etching solvent at ratio (1:1) in volume, etched at 60 min.

	White light	UV-254nm	UV-366nm
Single Cell			
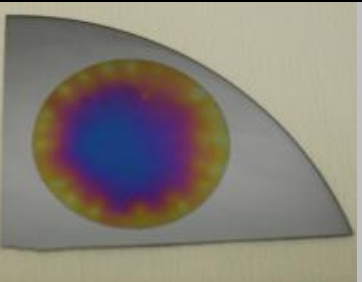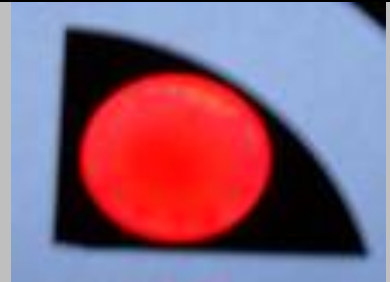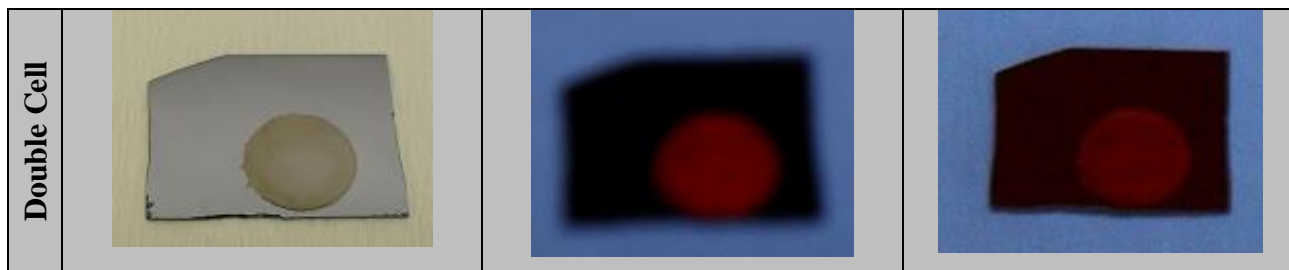
As a comparison, the UV PL emission of porous silicon samples prepared by controlling three specific alcoholic solvents and two electrochemical cells at constant etched time are shown in tables 2, 3 and 4. From the above tables we can notice a clear difference in the UV PL emission, despite the fact both cells have the same type of pores for (MeOH and PrOH alcohols) but this slight difference in sizes (width and depth) in few nanometers scale and in case of EtOH alcohol, formation of macropores fill of mespores, could be seen clearly reflected in the UV PL emission of both cells. This evident difference could be attributed to the structural factors related to the electrochemical cell design, volume of the cell (larger volume of the electrolyte is more accurate for homogeneous etching), distant of the counter electrode from the working electrode, kind of etching (vertical in case of single tank, horizontal in case of double tank), electrolyte composition (HF concentration, alcohol concentration), current density and anodization time[54-59].

3.3 I–V characteristics

I-V curve characterization has been used to inspect the pore formation in porous silicon layers. The current–voltage (I-V) characteristics of the PS samples without any treatment prepared by utilizing two electrochemical cells with two alcoholic solvents at constant etched time and current density are shown in figure 5.
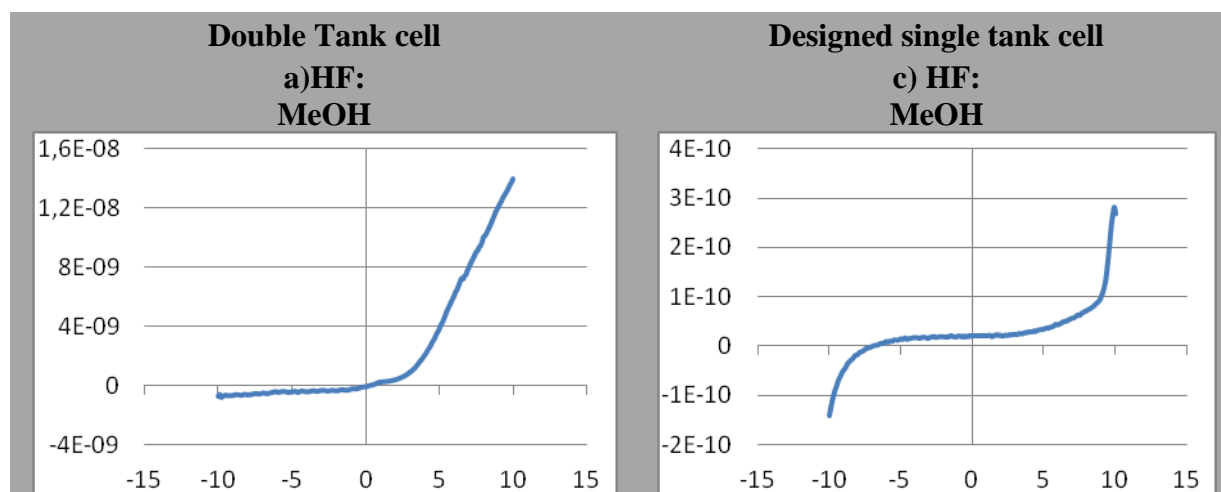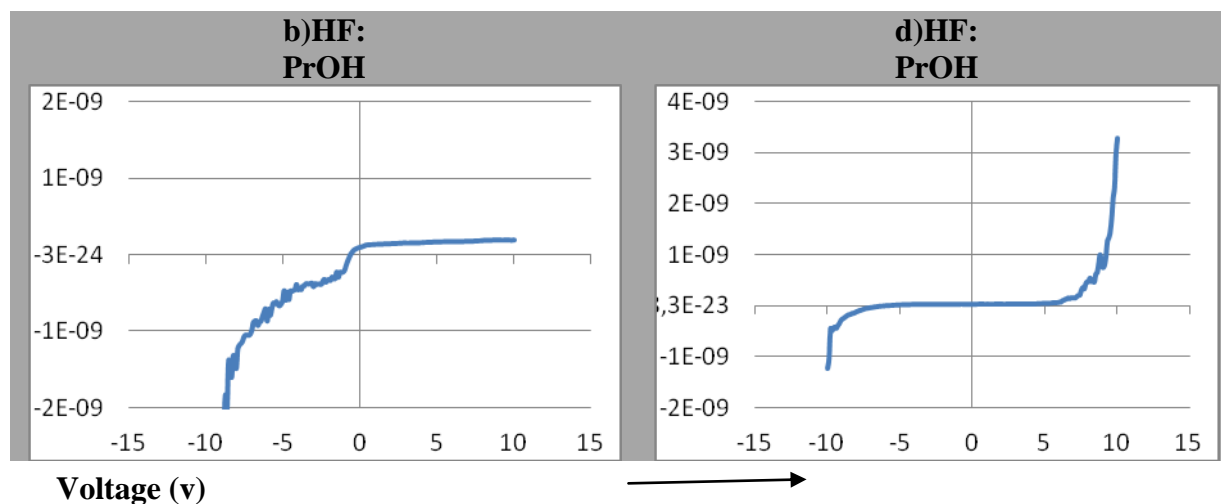
Figure 5. I-V measurement performed on prepared PS samples by using double tank cell (a)-(b), and designed single tank cell (c)-(d), with two different alcoholic solvents at current density 30mA/cm^2 and etched time 60 mint.

Fig.5 (a) the I-V curve of PS sample prepared by using double tank cell with HF:MeOH solution shows good agreement to the experimental I-V response of the characteristics of the previous reports [46,47]. Whilst, Fig. 5(b) the I-V curve of PS sample prepared with HF:PrOH solution shows different behavior in which we could notice, as the potential is increased; the current exhibits a peak and then remains at a relatively constant value[37] .

Fig.5 (c) and (d) show the I-V curves of PS samples prepared by using designed single tank cell with HF:MeOH and HF:PrOH . Their behavior show basic similarity to the normal Schottky diode behavior expected from a semiconductor/electrolyte interface, but there are some important differences[45, 48]. Electropolishing region does not occur in anhydrous organic solutions due to the lack of water which is required for the formation of oxide film [37].

Accordingly, it is believed that the design of the electrochemical cell has a significant effect on the pore formation. Not only current density or concentration of HF solution but also the type of alcohol and the etch cell engineering affects the morphologies, I-V characteristics and the UV PL emission.

4. CONCLUSION

From the above results and to the best of our knowledge and depending on the recent literatures there is not any research has been reported about the actual difference between the two electrochemical cells design (*designed* single tank cell and double tank cell) in the matter of anodization parameters effect. For both etching cells, three main types of pores were obtained, in spite of the difference in the diameters and depths of pores were: mesopores, mesopore fill of mesopores, and macropore fill of mesopores. PS samples exhibited strong and stable red-orange UV PL emission increases with increasing carbon numbers in the alcohol for *designed single tank cell* at room temperature than *double*

tank cell . Furthermore, the current–voltage (I-V) measurement showed basic similarities to the normal Schottky diode behavior.

References

1. R. Osorio-Saucedo, C .Vazquez-Lopez, W. Calleja, D.D. Allred and C. Falcony, *Thin Solid Films*, 338 (1999) 100.
2. A.Uhlir, *Bell Syst. Tech. J.*, 35(1956) 333.
3. R. Guerrero Lemus, J. D. Moreno, J. M. Martínez Duart and J. L. Corral, *Rev. Sci. Instrum.* , 67(1996)3627.
4. S. Shih, C. Tsai, K.-H. Li, H. H. Jung, J. C. Campbell and D. L. K.wong, *Appl. Phys. Lett.,* 60 (1992) 633.
5. A.Halimaoui, "Porous silicon: material processing, properties and applications" in *Porous Silicon Science and Technology,* J.-C Vial and J. Derrien, Eds. *,* Springer, Berlin, (1995).
6. A. G. Cullis, L. T. Canham and P. D. J. Calcott, *J. Appl. Phys.*, 82 (1997) 909.
7. M. J. Sailor, *Porous Silicon in Practice: Preparation, Characterization and Applications*, Wiley, Germany, 2012.
8. C.Becker, L.Currano and W.Churaman, *A.R.L.*, TR-4717(2009)1.
9. D.H.Ge, M.C.Wang, W.J.Liu, S.Qin, P.L. Yan and J.W.Jiao, *Electrochim.Acta*, 88 (2013) 141.
10. A. Loni, T. Defforge, E. Caffull, G. Gautier and L.T. Canham, *Micropor. Mesopor. Mat.,* 213(2015)1.
11. T. Urata, K. Fukami, T. Sakka and Y. H. Ogata, *N. R. L.,* 7:329 (2012)1.
12. J.H.Song and M.J. Sailor, *Inorg.Chem.,* 37 (1998) 3355.
13. M .Christophersen, J.Carstensen, K.Voigt and H. Föll , *Phys. Status Solidi A*,197(2003)34.
14. S. Matthias, F. Müller, C. Jamois, R.B. Wehrspohn and U. Gösele, *Adv. Mat.*, 16 (2004) 2166.
15. S. Mor, V. Torres-Costa, R.J. Martin-Palma and I. Abdulhalim, *Appl. Phys. Lett.*, 97(2010)113106.
16. W. Lang, *Mat.Sci.Eng.R.*, 17 (1996) 1.
17. J. Olivares, M. Clement, S. González-Castilla, L. Vergara, E. Iborra and J. Sangrador, *Thin Solid Films*, 518 (2010) 5128.
18. M. Thönissen, S. Billat, M. Krüger, H. Lüth, M.G. Berger,   U. Frotscher and U. Rossow, *J. Appl. Phys.,* 80 (1996) 2990.
19. H.-J. Kim, Y.-Y. Kim, K.-W. Lee and S.-H. Park, *Sensor. Actuat. B: Chem.*, 155 (2011)673.
20. V. Depauw, O. Richard, H. Bender, I. Gordon, G. Beaucarne, J. Poortmans, R. Mertens and J.-P. Celis, *Thin Solid Films*, 516 (2008) 6934.
21. P. Vitanov, E. Goranova, V. Stavrov, P. Ivanov and P.K. Singh, *Sol. Energ. Mat. Sol. C.*, 93 (2009) 297.
22. A.Benilov, M.Cabrera, V.Skryshevsky and J.-R. Martin, *Mat. Sci. Eng. B* ,139 (2007) 221.
23. J.-H. Park, L.Gu, G. von Maltzahn, E. Ruoslahti, S.-N. Bhatia and M.J. Sailor, *Nature Mater.*, 8 (2009) 331.
24. L.M. Bonanno and E. Segal, *Nanomedicine*, 6 (2011) 1755.
25. A.G. Cullis and L.T. Canham, *Nature* ,353 (1991) 335.
26. L.T. Canham, *Appl. Phys. Lett.,* 57 (1990) 1046.
27. M.J. Sailor and E.J. Lee, *Adv. Mater.*, 9 (1997) 783.
28. S. Ossicini, L. Pavesi and F. Priolo, *Light Emitting Silicon for Microphotonics*, Springer-Verlag, Berlin, 2003.
29. J. Lin, G.Q. Yao, J.Q. Duan, G.G. Qin, *Solid State Commun.*, 97 (1996) 221.
30. G.G. Qin, J. Lin, J.Q. Duan and G.Q. Yao, *Appl. Phys. Lett.*, 69 (1996) 1689.
31. Y. Zhang, Z. Yang, D.Liu, E.Nie, X.Bai, Z.Li, H.Song, Y. Zhou, W.Li, M.Gong and X.Sun, *J.Lumin.*, 130 (2010) 1005.

32. Y. SuPing, J. Kun, Z. Ke, H.WenXuan, D. Hai, L.MiaoChun and P.WenMing, *Chinese Sci. Bull.,* 56 (2011) 2706.
33. Veeco Instruments Inc. Nanocope Software 6.13 User Guide, 2002
34. F. A. Bruening and A. D. Cohen, *Int. J. Coal Geol.*, 63(2005)195.
35. M. H. Fadzilah Suhaimi, M. Ain Zubaidah, S. F. M. Yusop, M. Rusop and S.Abdullah, *IEEE-ICSE2012 Proc., 2012*, Kuala Lumpur, Malaysia
36. H. Song, Z. Li, H. Chen, Z.Jiao,Z.Yu,Y.Jin,Z.Yang,M.Gong and X.Sun, *App. Surf. Sci.* 254 (2008) 5655.
37. G. X. Zhang, "Porous Silicon: Morphology and Formation Mechanisms", in *Modern Aspects of Electrochemistry*, C. G. Vayenas, R. E. White, and M. E. Gamboa-Adelco, Eds., pp.65-133*,* Springer, New York, 2006
38. X.G.Zhang , *Electrochemistry of Silicon and Its Oxide*, Springer, New York, 2001.
39. C. M. Gronet, N. S. Lewis, G. Cogan and J. Gibbons, *Proc. Natl. Acad. Sci. USA* ,80(1983)1152.
40. V. Lehmann and S. Ronnebeck, *J. Electrochm.Soc.,* 146 (1999) 2968.
41. M. Christophersen, J. Carstensen, A. Feuerhake and H. Föll, *Mater.Sci.Eng,* B69-70 (2000) 194.
42. H.Kim and N.Cho , *N.R.L.,*7:408(2012)1.
43. V. Lehmann and U.Gosele, *Appl. Phys. Lett.*, 58(1991) 856.
44. A.J.Read, R. J.Needs, K.J.Nash, L.T. Canham, P.D.J. Calcott and A.Qteish, *Phys. Rev. Lett.*, 69(1992) 1232.
45. R. L. Smith and S. D. Collins, *J. Appl. Phys,* 71(1992) R1.
46. Z. B. Achour, O. Touayar andN. Sifi, *Modern Instrumentation*, 1 (2012)21.
47. M. Atyaoui, W. Dimassi , M. Khalifa, R.Chtourou and H.Ezzaouia, *J. Lumin*, 132 (2012) 2572.
48. O. Bisi, S. Ossicini and L. Pavesi, *Surf. Sci.Rep.,* 38 (2000) 1.
49. P. Williams, C. L´evy-Cl´ement, J.-E. P´eou, N. Brun, Ch. Colliex, R. Wehrspohn, J.-N. Chazalviel and A. Albu-Yaron, *Thin Solid Films*, 298 (1997) 66.
50. P.D.J. Calcott, K.J.Nash, L.T. Canham, M.J. Kane and D.Brumhead, *J. Lumin.*, 57(1993) 257.
51. K.J.Nash, P.D.J. Calcott, L.T.Canham and M.J. Kane*, J. Lumin.*, 60–61 (1994)297.
52. F. Buda, J. Kohanoff and M. Parrinello, *Phys. Rev. Lett.*, 69(1992)1272.
53. R.T. Collins and M.A.Tischler, *Circuits and Devices Magazine, IEEE,* 9(1993)22.
54. J. Jakubowicz, *Superlattice.Microst.*, 41 (2007) 205.
55. V. Lehmann and H. Föll, *J. Electrochem. Soc.*, 137 (1990) 653.
56. V . Lehmann, *Mater. Lett* ,28 (1996) 245.
57. V. Lehmann and U. Grüning, *Thin Solid Films*, 297 (1997) 13.
58. J. Carstensen, M. Christophersen and H. Föll, *Mat. Sci. Eng. B*, 69–70 (2000) 23.
59. G. Korotcenkov and B. K.Cho, *Crit. Rev. Solid State*, 35(2010)153.